JPEDAV (2004) 25:259-268
DOI: 10.1361/15477030419522
1547-7037/$19.00 ©ASM International

Thermodynamic Optimization of the Co-Zn System

George Penev Vassilev and Min Jiang

(Submitted 15 October 2001; in revised form 15 January 2004)

Literature information and authors' experimental data have been used for the evaluation of optimized polynomial coefficients serving to calculate the cobalt (Co)-zinc (Zn) phase diagram. The programs BINGSS and THERMO-CALC have been used for the optimization. The binary liquid phase, the solid Co-based face-centered-cubic (fcc) and hexagonal close-packed solutions, as well as the intermediate β-, β_1-, and γ-compounds have been treated as disordered substitutional phases. The phases with narrow homogeneity ranges (δ, γ_1, and γ_2) have been modeled as stoichiometric Co_2Zn_{15}, $CoZn_7$, and $CoZn_{15}$, respectively. The calculated phase diagram and thermodynamic quantities are in agreement with the experimental data. For the first time, a eutectoid decomposition (at around 658 K) of the fcc solutions has been predicted. Moreover, the calculations have shown the possibility for a magnetically induced miscibility gap involving both forms (paramagnetic and ferromagnetic) of the fcc solutions.

1. Introduction

Many of the experimental studies on the cobalt (Co)-zinc (Zn) phase diagram have been summarized by Hansen and Anderko [1958Han] and Massalski [1996Mas]. Previously, we have also performed numerous investigations of this phase diagram [1976Bud1, 1976Bud2, 1977Bud, 1977Vas, 1993Vas1, 1993Vas2]. Nevertheless, uncertainties concerning the phase boundaries and the thermochemical properties of this system persist.

The purpose of the present work was to achieve a thermodynamic optimization through a coupling phase diagram and thermochemical data for this system. The programs BINGSS [1995Luk] and THERMO-CALC have been used for this purpose.

2. Experimental Information

2.1. Phase Diagram and Structure Data

The contemporary notations and data concerning the crystal structures of the solid binary phases in the Co-Zn system are compiled in Table 1.

2.1.1 Liquidus and Solidus. Lewkonja [1908Lew] as well as Pierce and Palmerton [1923Pie] were the first to study the equilibrium between the liquid and the solid phases in the Zn-rich region; they found eutectic invariants at 686 K and at 692 K, respectively. Detailed investigations of the phase equilibria between the liquid solutions and the intermediate phases have been performed by Schramm [1938Sch1, 1941Sch]. The high-temperature liquidus and solidus lines, in the interval 10-63 at.% Zn have been constructed by Budurov and Vassilev [1976Bud1].

George Penev Vassilev, University of Sofia, Faculty of Chemistry, 1 J. Bourchier Avenue, 1164 Sofia, Bulgaria; and **Min Jiang,** Department of Materials Science, Graduate School of Engineering, Tohoku University, Sendai 980-8579, Japan. Contact e-mail: gpvassilev@excite.com.

2.1.2 The Solvus of the Co-Based Solid Solutions: fcc-Co,Zn or α-Co,Zn Phase and Hexagonal Close-Packed-Co,Zn or ε-Co,Zn Phase. Schramm [1938Sch3, 1941Sch] reported a diminishing Zn solubility in (α-Co) from 1223 K to 673 K. He studied the magnetic transition in these alloys as well [1938Sch4]. Takayama et al. [1995Tak] have recently reinvestigated the solvus, emphasizing the influence of the magnetic transition on its shape. The latter authors' data, below the Curie temperature (T_C), differ from those of Schramm [1941Sch] deviating toward lower Zn solubility.

It is known [1987Gui, 1990Nis, 1991Ray] that, during heating, the pure hexagonal close-packed Co (HCP-Co or ε-Co) undergoes a polymorphic transition at about 695 K and converts to its high-temperature form [face-centered-cubic (fcc)-Co or α-Co]. There are discrepancies in the literature concerning the influence of Zn additions on the transition temperature. According to Köster and Wagner [1937Kos], the (ε-Co) → (α-Co) transition temperature increases with Zn content, while the transition temperature of the reverse reaction (α-Co) → (ε-Co) diminishes. On the contrary, Hashimoto [1937Has] has observed that both temperatures increase with increasing Zn concentration. Köster and Schmid [1955Kos] have confirmed the observation of Hashimoto [1937Has]. In the present work, the latter results have been accepted, as well as the Zn solubility in (ε-Co) determined by Lihl and Weisberg [1955Lih] (2.5 at.% at 573 K).

2.1.3 β and β_1 Intermediate Phases. These electronic compounds exist in the equiatomic region of the phase diagram. The β_1-phase is ferromagnetic below 398 K [1938Sch3, 1941Sch, 1958Han, 1951Mey], but no details about the concentration dependence of the T_C are known.

The β- and β_1-phase boundaries have been studied by Schramm [1938Sch1, 1938Sch2, 1938Sch3] using thermoanalytical, microscopic, and x-ray methods. They were reinvestigated later [1955Lih, 1955Kos] and diminishing Co solubility in the β_1-phase was revealed.

In most phase diagram compilations [1958Han, 1996Mas], the β_1/γ-phase boundary has been considered to be vertical, but there are contradictions concerning the β_1-phase homogeneity interval. At 298.15 K, the interval is

Table 1 Crystal Structures of the Solid Binary Phases in the Co-Zn System

Phase	Pearson Symbol	Space Group	Struckturbericht Designation	Prototype	Reference
α, (αCo) (a)	*cF*4	$Fm\bar{3}m$	*A*1	Cu	1941Sch
ε, (εCo) (b)	*hP*2	$P6_3/mmc$	*A*3	Mg	1955Lih
β (CoZn) (c)	*cI*2 or? *cP*2	$Im\bar{3}m$	*A*2 (disordered)	W	1938Sch3
		$Pm\bar{3}m$	*B*2 (ordered)	CsCl	
β_1(CoZn) (a)	*cP*20	$P4_132$	*A*13	βMn	1932Par; 1931Ekm 19381Sch3 1983Bus
γ (Co_5Zn_{21})	*cP*52	$P\bar{4}3m$	$D8_3$	Cu_9Al_4	1955Lih
γ (Co_5Zn_{21})	*cI*52	$I\bar{4}3m$	$D8_{1\text{-}3}$	Cu_5Zn_8	1931Ekm; 1932Par 1938Sch3 1996Rya
γ_1 ($CoZn_7$)	(d)	Cubic	(d)	γ-brass related	1941Got
γ_2 ($CoZn_{13}$)	*mC*28	*C*2/m	(d)	$CoZn_{13}$	1962Bro
δ (c) approx. Co_2Zn_{15}	(d)	(d)	(d)	(d)	(d)
η, (ηZn)	*hP*2	$P6_3/mmc$	*A*3	Mg	1923Pie; 1938Sch1

(a) Phases where magnetic transitions occur
(b) Ferromagnetic phase
(c) High-temperature phases
(d) No data available

53.0-53.8 at.% Zn according to the compilations of Hansen and Anderko [1958Han] and Massalski [1996Mas], while Lihl and Weisberg [1955Lih] have found that it is in the interval 55.5-59.0 at.% Zn at 573 K. According to Köster and Wagner [1937Kos], the maximal Zn solubility in the β_1-phase is 56.9 at.%. All of these authors agree that the Co content in the β_1-phase increases with increasing temperature. However, Takayama et al. [1995Tak] have suggested that both β_1-phase boundaries are vertical, comprising the range from 47.5-57.3 at.% Zn. It seems, however, that the shape of the β_1/α-phase boundary is more complicated, reflecting the Gibbs energy (G) changes due to the magnetic and allotropic transitions.

In connection with these uncertainties, we performed experiments to obtain more data about the low-temperature phase equilibria. Alloys have been studied by the annealing of weighted mixtures, sealed under vacuum, in silica tubes. Scanning electron microscopy has been applied to determine the compositions. In specimen 1 (overall Zn content 44.2 at.% Zn), annealed for 22 days at 807 °C and for 96 days at 387 °C, β_1- and γ-phase diffusion layers have been observed around a single non-reacted Co particle. We consider the finding that Co-rich precipitation has been observed in the β_1-phase, indicating that the β_1/α-phase boundary is not vertical, to be very interesting. The Co-rich phase has a Zn content that is much higher (>20 at.%) than the expected one, but the probable reason is that the full thermodynamic equilibrium has not been achieved yet and the observed solid solution is metastable (Fig. 1). Our general impression from previous and present studies is that the transformation from the high-temperature fcc structure to the low-temperature HCP is sluggish. This could be due to the existence of a metastable miscibility gap (i.e., a low-temperature continuation of the magnetically induced miscibility gap, with an invariant reaction at around 1015 K).

The Zn concentrations at the diffusion layer phase boundaries (in which X_{Zn} is the Zn mole fraction) are as follows: X_{Zn} (γ/β_1) = 0.720; X_{Zn} (β_1/γ) = 0.600; and X_{Zn} (β_1/α) = 0.495.

In specimen 2, which was annealed for 21 days at 825 °C and for 96 days at 299 °C (overall composition X_{Zn} = 0.649), the following phase boundary concentrations have been observed: X_{Zn} (γ/β_1) = 0.716; X_{Zn} (β_1/γ) = 0.561; and X_{Zn} (β_1/α) = 0.472. Yet again, the concentration at the boundary between the β_1-layer and the Co-rich phase strongly deviates from the expected equilibrium value, while the compositions of the intermetallic layers are within expected concentration intervals. One should be aware that the concentrations read at the phase boundaries of diffusion layers might be different, to some extent, from those of the equilibrium. However, our results are in general agreement with the higher temperature data of Takayama et al. [1995Tak].

2.1.4 γ-, γ_1-, γ_2-, δ-, and (ηZn)-Phases. The γ-phase can be regarded as consisting of Co or Zn solid solutions based on the compound Co_5Zn_{21} [1931Ekm, 1932Par] with variable numbers of atomic species per unit cell [1973Mel, 1996Rya], which is analogous to γ-brass. Indeed, its structure is of γ-brass type [1937Kos, 1955Lih, 1996Rya] (Table 1). Thus, it is a typical electronic compound, and the important role of the electron concentration for its stability has been proven [1977Mor].

The γ_1- and γ_2-phases have narrow homogeneity ranges and structures that are similar to that of the γ-phase [1938Sch3, 1941Got, 1962Bro]. A monoclinic cell has been attributed later for the γ_2-phase ($CoZn_{13}$) [1932Par, 1951Mey, 1973Mel].

The δ-phase decomposes peritectically (Table 3) at 948 K [1958Han, 1996Mas], and no information about its structure could be found. Both the γ_1- and δ-phases might

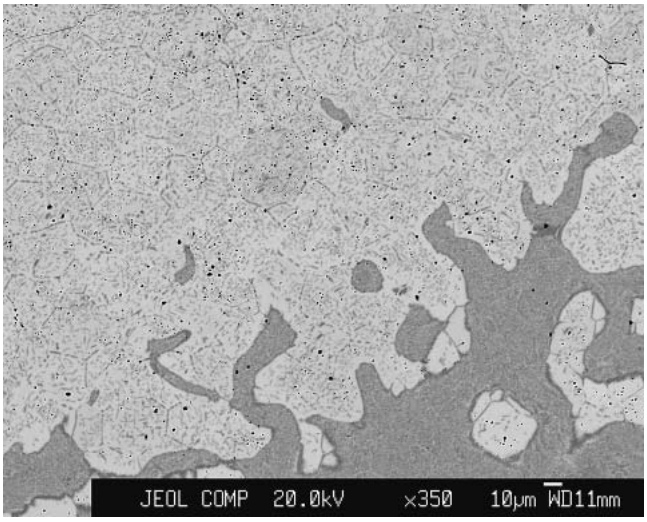

Fig. 1 Micrograph of specimen 1 in characteristic x-rays. The dark areas represent Co-Zn solid solutions (21.9-30.7 at.% Zn) and the light-gray areas represent the β_1-phase (51.2-53.5 at.% Zn). The dark precipitations along the grain boundaries belong to the Co-Zn solutions as well. The specimen was annealed first at 807 °C and thereafter at 387 °C.

have some homogeneity ranges corresponding roughly to the stoichiometry $CoZn_{(7\text{-}9)}$.

We have identified layers of γ-, γ_1-, and γ_2-phases in a study of intermediate-phase growth kinetics using metallographic, microhardness, x-ray, and electron microprobe analyses [1993Vas2]. Nevertheless, in the latter work the homogeneity ranges were not studied.

The (ηZn) has the same structure as the HCP-Co, but the Co solubility in this phase is not well-determined. Anyhow, it is clear that it is rather small [1944Paw].

2.2. Thermodynamic Data

2.2.1 Liquid Phase and Terminal Solid Solutions (ηZn,Co, αCo,Zn, and εCo,Zn). The Zn activities in the binary liquid solutions at 1813 K (0.0083-0.0281 mole fraction of Zn) have been studied by Mozeva et al. [1977Moz] applying the isopiestic method. Due to the narrow composition interval and method restriction, those data were not very useful. The extrapolated data of Comert and Pratt [1982Com] at 1023 K and high Zn content are known as well (Fig. 2).

The thermodynamic properties of the solid fcc Co-Zn solutions, in the range 693-833 K, have been investigated by Ali and Geiderich [1981Ali] [electro-motive force measurements (EMF) with molten electrolytes]. Later, Budurov et al. [1976Bud2] studied the Zn activities, at 1086 and 1296 K, by the dew-point method, while Comert and Pratt [1982Com] worked on the interval 873-1173 K (EMF with solid electrolytes) (Fig. 3).

No experimental data about the thermodynamics of the solid HCP solutions (ε-Co and η-Zn phases) are available, as far as we know.

2.2.2 Intermediate (β, β_1, γ, γ_1, γ_2, and δ) Phases. Comert and Pratt [1982Com] have determined the thermodynamic properties of the β_1-phase (Fig. 4) and the γ-phase (Fig. 5). Ali and Geiderich [1981Ali] have measured the Zn activities in the β_1-phase (Fig. 4) and γ-phase (Fig. 5). Budurov and Vassilev [1977Bud] using the dew-point

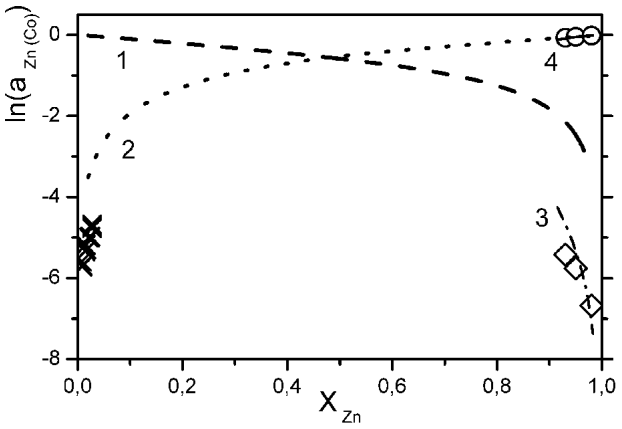

Fig. 2 Experimental and calculated Zn and Co activities (referred to as the liquid Zn and liquid Co, respectively) in the binary liquid solutions. X represents Zn activities measured by Mozeva et al. [1977Moz] at T = 1813 K. Comert and Pratt [1982Com] extrapolated Zn (○) and Co (◇) activities at T = 1023 K. Lines 1-4 represent values calculated in this work as follows: lines 1 and 3, Co activities at 1800, 1600, and 1023 K, respectively; lines 2 and 4, Zn activities at 1800 and 1023 K, respectively. The natural logarithms of the Zn and Co activities [$\ln(a_{Zn})$, $\ln(a_{Co})$] are plotted along the ordinate, and the mole fraction of Zn (X_{Zn}) is plotted along the abscissa.

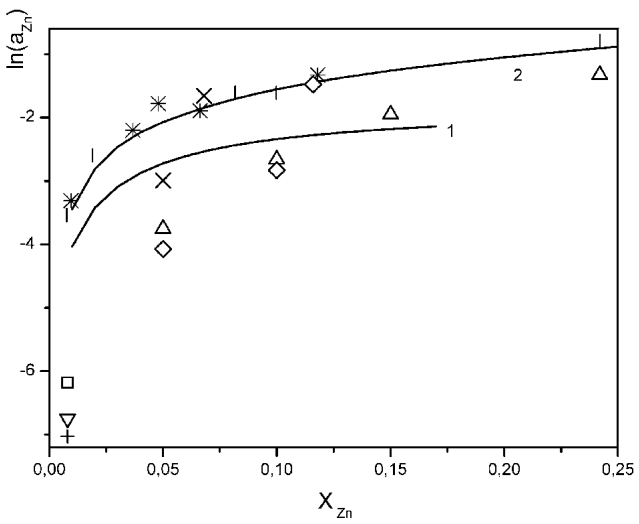

Fig. 3 Measured and calculated Zn activities (referred to the liquid Zn) in the Co-Zn fcc solutions: I and *, Budurov et al. [1976Bud] at 1086 and 1296 K, respectively; Δ, ◇, and ×, Comert and Pratt [1982Com] at 1023. 973 and 923 K; +, ∇, and □, Ali and Geiderich [1981Ali] at 700, 730 and 760 K. The lines represent the Zn activities calculated in this work: 1, at 700 K; and 2, at 1300 K The natural logarithms of the Zn activities [$\ln(a_{Zn})$] are plotted along the ordinate and the mole fraction of Zn (X_{Zn}) along the abscissa.

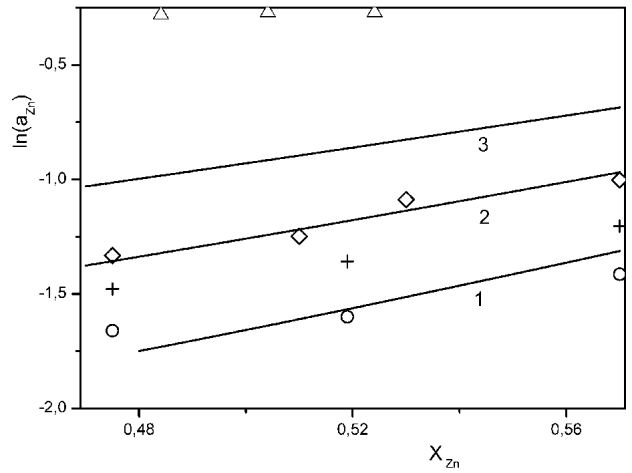

Fig. 4 Measured and calculated Zn activities (referred to the liquid Zn) in the Co-Zn β_1-phase: Δ, Budurov and Vassilev [1977Bud] at 1073 K; ◊, Δ, and ○, Comert and Pratt [1982Com] at 1023, 973, and 923 K, respectively; +, Ali and Geiderich [1981Ali] at 1073 K. The lines represent the values calculated in this work: 1, at 923 K; 2, at 1023 K; and 3, at 1123 K. The natural logarithms of the Zn activities [$\ln(a_{Zn})$] are plotted along the ordinate, and the mole fraction of Zn (X_{Zn}) is plotted along the abscissa.

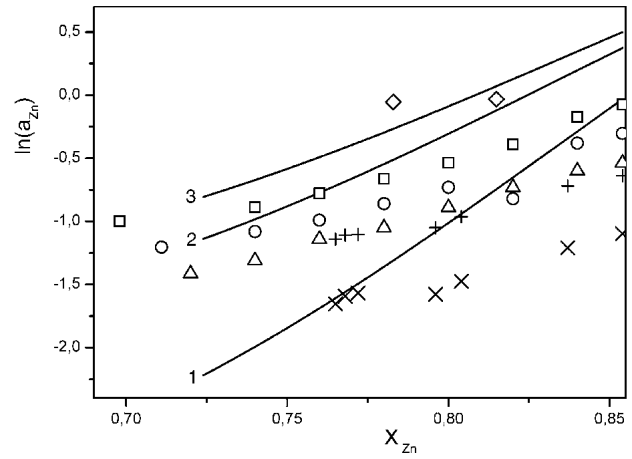

Fig. 5 Measured and calculated Zn activities (referred to the liquid Zn) in the Co-Zn γ-phase: ◊, Budurov and Vassilev [1977Bud] at 1073 K; □, ○, and Δ, Comert and Pratt [1982Com] at 1023, 973, and 923 K, respectively; + and ×, Ali and Geiderich [1981Ali] at 825 K and 700 K, respectively. The lines represent the data calculated in this work: 1, at 700 K; 2, at 923 K; and 3, at 1023 K. The natural logarithms of the Zn activities [$\ln(a_{Zn})$] are plotted along the ordinate, and the mole fraction of Zn (X_{Zn}) is plotted along the abscissa.

method, obtained the Zn activities for the β_1- and γ-phases for temperatures in the region 960-1100 K.

Calorimetric measurements of the enthalpies of formation for those alloys are not available, but some estimations have been done by both Comert and Pratt [1982Com] and Ali and Geiderich [1981Ali] using their own experimental results (Fig. 6).

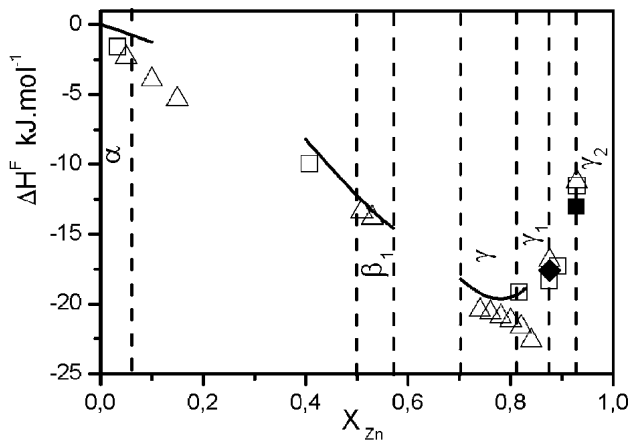

Fig. 6 Integral molar enthalpies of formation (ΔH^F kJ · mol^{-1}) of the solid cobalt-zinc alloys, calculated in this work for 800 K (the solid lines for α-, β_1- and γ-phases; the symbols ◆ and ■ for γ_1 and γ_2 phases, respectively), compared with temperature-independent assessed values of Comert and Pratt [1982Com] (Δ); and of Ali and Geiderick [1981Ali] (□). The zinc mol fractions (X_{Zn}) are plotted along the abscissa. The dashed lines represent the approximated phase boundaries at 800 K. The reference states are the fcc Co and the liquid Zn.

3. Thermodynamic Modeling and Optimization

3.1. Previous Thermodynamic Calculations

Previous modeling of the thermodynamic properties of the α-phase and liquid phase has been done by Vassilev [1993Vas1], and the equilibrium lines between both solutions have been calculated.

3.2. Analytical Description of the Gibbs Energies

3.2.1 Elements. A detailed study of the Co phase stabilities has been performed by Guillermet [1987Gui]. These descriptions have been retained in the compilation of Dinsdale [1991Din]. The temperature dependencies of the molar G values (^0G_i) for the pure elements are described in the form:

$$^0G_i(T) - {}^0H_i^{SER} = A_i + B_iT + C_iT\ln T + D_iT^2 + E_i/T + F_iT^3 + I_iT^4 + J_iT^7 + K_iT^{-9} + \Delta G_{mag}(T) \quad \text{(Eq 1)}$$

where $^0H_i^{SER}$ represents the enthalpy of the pure element i, in its stable state, at the standard temperature 298.15 K and a pressure of one bar, T is the temperature of interest, and $\Delta G_{mag}(T)$ is the magnetic term. The coefficients A_i through K_i for pure Co are taken from the special group of thermodynamic equilibria Europe (SGTE) data file [1991Din] (Table 2). The paramagnetic states of the pertinent phases are taken as references, and the magnetic contribution (ΔG_{mag}) is treated separately [1978Hil, 1981Ind, 1995Luk].

The pertinent coefficients for the pure Zn given by Dinsdale [1991Din] are updated following Kowalski and Spencer [1993Kow] and Vassilev et al. [2000Vas] (Table 2).

Table 2 Thermodynamic Database File for Calculation of the Co-Zn Phase Diagram

Element stable element reference mass		H298-H0	S298
−1/−ELECTRON_GAS	0.0000EE+00	0.0000E+00	0.0000E+00
0 VA VACUUM	0.0000E+00	0.0000E+00	0.0000E+00
1 CO HCP_A3	5.8933E+01	4.7656E+03	3.0040E+01
2 ZN HCP_A3	6.5380E+01	5.6567E+03	4.1631E+01

Function GHSERCO
298.14 < T < 1768.00: +310.241 + 133.36601*T − 25.0861*T*LN(T)
−.002654739*T**2 − 1.7348E-07*T**3 + 72 527*T**(−1)
1768.00 < T < 6000.00: −17 197.666 + 253.28374*T − 40.5*T*LN(T)
+9.3488E + 30*T**(−9)

Function GCOFCC
298.14 < T < 1768.00: + 737.832 + 132.750762*T − 25.0861*T*LN(T)
−.002654739*T**2 − 1.7348E-07*T**3 + 72 527*T**(−1)
1768.00 < T < 6000.00: − 16 770.075 + 252.668487*T − 40.5*T*LN(T)
+9.3488E+30*T**(−9)

Function GCOBCC
298.14 < T < 3000.00: +2937.831 − .7138*T + GHSERCO

Function GCOLIQ
298.14 < T < 1768.00: + 15 395.278 + 124.434078*T − 25.0861*T*LN(T)
−.002654739*T**2-1.7348E − 07*T**3 + 72 527*T**(−1)
1768.00 < T < 6000.00: −846.61 + 243.599944*T − 40.5*T*LN(T)

Function GCOA13
298.14 < T < 3000.00: +3155 + GHSERCO

Function GHSERZN
298.14 < T < 692.68: −7285.787 + 118.469269*T
−23.701314*T*LN(T)
−.001712034*T**2−1.264963E−06*T**3
692.68 < T < 6000.00: −11 070.597 + 172.344911*T − 31.38*T*LN(T)
+4.70657E + 26*T**(−9)

Function GZNFCC
298.14 < T < 3000.00: +2969.82 − 1.56968*T + GHSERZN

Function GZNBCC
298.14 < T < 3000.00: +2886.96 − 2.5104*T + GHSERZN

Function GZNLIQ
298.14 < T < 692.73: +7157.27 − 10.292343*T − 3.5865E
− 19*T**7 + GHSERZN
692.73 < T < 3000.00: +7450.123 − 10.736234*T − 4.7066E
+ 26*T**(−9) + GHSERZN

Phase LIQUID
Excess model is Redlich-Kister_Muggianu
Constituents: CO,ZN
G(LIQUID,CO;0)-H298(HCP_A3,CO;0) = +GCOLIQ
G(LIQUID,ZN;0)-H298(HCP_A3,ZN;0) = 298.14 < T < 3000.00:
+GZNLIQ
L(LIQUID,CO,ZN;0) = −15 017 + 12.735*T
L(LIQUID,CO,ZN;1) = +51 758 − 29.752*T

Phase BETA1
Excess model is Redlich-Kister_Muggianu
Additional contribution from magnetic ordering p = 0.400
2 Sub-lattices, Sites 1:1
Constituents: CO,ZN:VA
G(BETA1,CO:VA;0)-H298(HCP_A3,CO;0) = +GCOBCC
TC(BETA1,CO:VA;0) = 1450
BMAGN(BETA1,CO:VA;0) = 1.35
G(BETA1,ZN:VA;0)-H298(HCP_A3,ZN;0) = +GZNBCC
TC(BETA1,CO,ZN:VA;0) = −861
L(BETA1,CO,ZN:VA;0) = −60 380 + 41.475*T
L(BETA1,CO,ZN:VA;1) = +48 088 − 30.451*T

Phase BETA
Excess model is Redlich-Kister_Muggianu
2 Sub-lattices, Sites 1:1
Constituents: CO,ZN:VA
G(BETA,CO:VA;0)-H298(HCP_A3,CO;0) = +GCOBCC
G(BETA,ZN:VA;0)-H298(HCP_A3,ZN;0) = +GZNBCC
L(BETA,CO,ZN:VA;0) = −33 588 + 19.099*T
L(BETA,CO,ZN:VA;1) = +15 504 − 2.971*T

Phase DELTA
2 Sub-lattices, Sites .117647: .882353
Constituents: CO:ZN
G(DELTA,CO:ZN;0)-0.1176471 H298(HCP_A3,CO;0) − 0.8823529
H298(HCP_A3,ZN;0) = −7494 + .1176471*GHSERCO
+ .8823529*GHSERZN

Phase FCC_A1
Excess model is Redlich-Kister_Muggianu
Additional contribution from magnetic ordering p = 0.280
2 Sub-lattices, Sites 1:1
Constituents: CO,ZN:VA
G(FCC_A1,CO:VA;0)-H298(HCP_A3,CO;0) =+GCOFCC
TC(FCC_A1,CO:VA;0) = 1396
BMAGN(FCC_A1,CO:VA;0) = 1.35
G(FCC_A1,ZN:VA;0)-H298(HCP_A3,ZN;0) = +GZNFCC
L(FCC_A1,CO,ZN:VA;0) = −34 275 + 23.006*T
L(FCC_A1,CO,ZN:VA;1) = +18 019 + −9.93800*T
TC(FCC_A1,CO,ZN:VA;0) = −332

Phase GAMMA1
2 Sub-lattices, Sites .125: .875
Constituents: CO:ZN
G(GAMA1,CO:ZN;0)-0.125 H298(HCP_A3,CO;0) − 0.875
H298(HCP_A3,ZN;0) = −12 051 + 4.52*T + .125*GHSERCO
+ .875*GHSERZN

Phase GAMMA2
2 Sub-lattices, Sites .0714286: .928571
Constituents: CO:ZN
G(GAMA2,CO:ZN;0)-0.0714286 H298(HCP_A3,CO;0)
− 0.9285714 H298(HCP_A3,ZN;0) = −6710 + 1.533*T
+ .0714286*GHSERCO + .9285714*GHSERZN

Phase GAMMA
Excess model is Redlich-Kister_Muggianu
2 Sub-lattices, Sites 1:1
Constituents: CO,ZN:VA
G(GAMMA,CO:VA;0)-H298(HCP_A3,CO;0) = +10000 + GHSERCO
G(GAMMA,ZN:VA;0)-H298(HCP_A3,ZN;0) = +10000 + GHSERZN
L(GAMMA,CO,ZN:VA;0) = −75 720 + 27.599*T
L(GAMMA,CO,ZN:VA;1) = +61 919 + 35.000*T
L(GAMMA,CO,ZN:VA;2) = −122 000 + 31.483*T

Phase HCP_A3
Excess model is Redlich-Kister_Muggianu
Additional contribution from magnetic ordering p = 0.280
2 Sub-lattices, Sites 1: .5
Constituents: CO,ZN:VA
G(HCP_A3,CO:VA;0)-H298(HCP_A3,CO;0) = +GHSERCO
TC(HCP_A3,CO:VA;0) = 1396
BMAGN(HCP_A3,CO:VA;0) = 1.35
G(HCP_A3,ZN:VA;0)-H298(HCP_A3,ZN;0) = +GHSERZN
L(HCP_A3,CO,ZN:VA;0) = −205 000 + 22.5*T
TC(HCP_A3,CO,ZN:VA;0) = −332

The temperature and composition values for the invariant reactions assessed by Hansen and Anderko [1958Han] and Massalski [1996Mas] have been used. However, there are no data concerning the low-temperature ternary equilibrium between α-, ε-, and β_1-phases, that by theoretical considerations, must exist in this system.

3.2.2 Solution Phases (α or fcc-Co,Zn, HCP-Co,Zn or εCo,Zn, and ηZn,Co, Liquid). These binary phases have been treated as disordered substitutional solutions in the same way as that described in the optimization of the Ni-Zn system [2000Vas].

It has been found that first-degree Redlich-Kister polynomials (equivalent to a sub-regular solution model) are sufficient to describe the optimized excess thermodynamic properties of the α- and liquid phases. For the hexagonal (HCP_A3) ε-phase, existing across a narrow concentration interval, a zero degree Redlich-Kister polynomial description (equivalent to a regular solution model) has been applied (Table 2). The ηZn,Co phase (also HCP_A3) has been assumed to be thermodynamically identical with εCo,Zn.

The magnetic contribution to the Gibbs energy descriptions of the α-, ε-, and β_1-phases was accomplished by the formalism of Inden [1981Ind] as modified by Hillert and Jarl [1978Hil]. It is based on Redlich-Kister type polynomials for both, the T_C, and the effective magnetic moment [1978Hil, 1981Ind, 1995Luk, 2000Vas]. We have assessed the pertinent coefficients (Table 2) following Takayama at al. [1995Tak], Hansen and Anderko [1958Han], and Massalski [1996Mas].

3.2.3 Nonstoichiometric Intermetallic Phases (β, β_1, and γ). The crystal structure of the high-temperature β-phase is probably of the B2 type, thus a two-sub-lattice description $[(Co,Zn)_1(Zn,Co)_1]$ could be applied. The β-Mn structure of the β_1-phase has two different Wyckoff positions, 8(c) and 12(d). Thus, the site fractions of the two sub-lattices must represent this ratio. Consequently, the model $(Co,Zn)_2(Zn,Co)_3$ would be adequate. However, as in the prototype β-Mn, both positions are equally occupied, so a Redlich-Kister description may be suitable for this phase as well. The latter model is applied to the β_1-phase, since differences between both sites are expected to be small.

It has been found (Table 1) that the ideal structural stoichiometry for the γ-phase is Co_5Zn_{21}. Detailed x-ray [1973Mel] and electron paramagnetic resonance studies

Table 3 Experimental or Estimated Data About the Invariants and the Special Points of the Co-Zn Phase Diagram Compared With the Calculated Values

Reaction Type	T (K)	$X^{LEFT\ SIDE}$	X^{MIDDLE}	$X^{RIGHT\ SIDE}$	Reference
Congruent melting Co(FCC) ↔ Co(L)	1768		0.00		1991Din, 1993Bar
Peritectic α + L ↔ β	1239	$X_\alpha = 0.375$	$X_\beta = 0.495$	$X_L = 0.640$	1958Han
	1239	$X_\alpha = 0.358$	$X_\beta = 0.495$	$X_L = 0.664$	Calculated
Peritectoid α + β ↔ β_1	1198	$X_\alpha = 0.375$	$X_{\beta_1} = 0.475$	$X_\beta = 0.495$	1958Han
	1198	$X_\alpha = 0.368$	$X_{\beta_1} = 0.502$	$X_\beta = 0.506$	Calculated
Peritectic L + β_1 ↔ β	1197	$X_{\beta_1} = 0.515$	$X_\beta = 0.535$	$X_L = 0.665$	1958Han
	1197	$X_{\beta_1} = 0.529$	$X_\beta = 0.532$	$X_L = 0.694$	Calculated
Peritectic L + β_1 ↔ γ	1168	$X_{\beta_1} = 0.538$	$X_\gamma = 0.690$	$X_L = 0.710$	1958Han
	1168	$X_{\beta_1} = 0.540$	$X_\gamma = 0.660$	$X_L =$	1995Tak
	1177	$X_{\beta_1} = 0.557$	$X_\gamma = 0.691$	$X_L = 0.716$	Calculated
Peritectic L + γ ↔ δ	1019	$X_\gamma = 0.845$	$X_\delta = 0.875$	$X_L = 0.931$	1958Han
	1168	$X_\gamma = 0.798$	$X_\delta = 0.882$	$X_L = 0.921$	Calculated
Peritectoid γ + δ ↔ γ_1	963	$X_\gamma = 0.854$	$X_{\gamma 1} = 0.875$	$X_\delta = 0.880$	1958Han
	961	$X_\gamma = 0.806$	$X_{\gamma 1} = 0.875$	$X_\delta = 0.882$	Calculated
Peritectic δ ↔ L + γ_1	948	$X_{\gamma 1} = 0.875$	$X_\delta = 0.90$	$X_L = 0.970$	1923Pie
	948	$X_{\gamma 1} = 0.875$	$X_L = 0.882$	$X_L = 0.961$	Calculated
Peritectic γ_1 + L ↔ γ_2	839	$X_{\gamma 1} = 0.9$	$X_{\gamma 2} = 0.917$	$X_L = 0.991$	1958Han
	840	$X_{\gamma 1} = 0.875$	$X_{\gamma 2} = 0.9285$	$X_L = 0.991$	Calculated
Eutectic L ↔ γ_2 + (Zn)	≈692.6	$X_\gamma = 0.9285$	$X_L > 0.997$	$X_{(Zn)} \approx 1$	1923Pie
	692.65	$X_\gamma = 0.9285$	$X_L \approx 0.9998$	$X_{(Zn)} \approx 1$	Calculated
Congruent melting Zn(s) ↔ Zn(L)	692.65		$X_{Zn} = 1.0000$		1993Bar
	692.73		$X_{Zn} = 1.0000$		1991Din, 1993Kow
Monotectoid (a) (αCo) (b) ↔ (αCo) (c) + β_1					
		No experimental data			
	1015	$X_{(\alpha Co)f} = 0.200$	$X_{(\alpha Co)p} = 0.234$	$X_{\beta_1} = 0.467$	Calculated
Eutectoid (αCo) ↔ (εCo) + β_1					
		No experimental data			
	658	$X_{(\varepsilon Co)} = 0.028$	$X_{(\alpha Co)} = 0.037$	$X_{\beta_1} = 0.525$	Calculated

(a) Critical point coordinates: $X_{Zn} = 0.184$, T = 1089
(b) Paramagnetic
(c) Ferromagnetic

Table 4 Experimental and/or Estimated Enthalpy Changes and Temperatures for the Invariants of the Co-Zn Phase Diagram Compared With Values Calculated in the Present Work

Equilibrium	Reaction (a)	Estimated T (K)	Experimental Enthalpy ($J \cdot mol^{-1}$)	Calculated T (K)	Calculated enthalpy ($J \cdot mol^{-1}$)
Zn(s) ↔ Zn(L)	C.M.	692.73	7 320	692.73	7 320
(αCo) ↔ (εCo) + β_1	E.D.	(b)	(b)	658.48	−690
(αCo) (c) ↔ (αCo) (d) + β_1	M.	(b)	(b)	1014.7	−1 180
L ↔ γ_2 + (Zn)	E.C.	≈692.6	(b)	692.66	−7 330
L + γ_1 ↔ γ_2	P.C.	839	(b)	840.25	−3 440
δ ↔ L + γ_1	P.C.	948	(b)	948.07	−3 070
γ + δ ↔ γ_1	P.R.	963	(b)	961.13	−3 850
L + γ ↔ δ	P.C.	1019	(b)	1016.49	−5 330
L + β_1 ↔ γ	P.C.	1168	(b)	1176.82	−14 660
β ↔ β_1 + γ	E.D.	1197	(b)	1197.00	−6 870
α + β ↔ β_1	P.R.	1198	(b)	1198.00	−6 720
α + L ↔ β	P.C.	1239	(b)	1238.95	−4 000
(αCo) ↔ Co(L)	C.M.	1768	16 200	1768	16 200

(a) C.M., congruent melting; E.D., eutectoid decomposition; E.C., eutectic crystallizaiton; P.C., peritectic crystallization; P.R., peritectoid recrystallization; M, monotectic
(b) No data available
(c) Paramagnetic state
(d) Ferromagnetic state

[1996Rya] have shown that it forms solid solutions with variable site occupancy by atoms and vacancies in the unit cell [1980Arn, 1982Pea]. In this case, the following distribution of the sites should be admitted: $(Co,Va)_5(Zn,Co)_{21}Co_5Zn_{21}$. This is similar to what was done for the Ni-Zn γ-phase [2000Vas]. We achieved a successful optimization using the latter model. Nevertheless, simplified models, without accounting for vacancies, recently have been preferred [2003Jia] because they facilitate the compatibility of various works when higher order systems are optimized for the development of thermodynamic databases. As the phase under consideration has a significant homogeneity interval, a simple substitutional solution model (Co,Zn) with full solubility in a single sub-lattice was chosen finally (Table 2).

3.2.4 Stoichiometric Phases (δ, γ_1, γ_2). Actually, these phases exhibit narrow concentration intervals [1958Han, 1996Mas]. Nevertheless, we have preferred to model them as stoichiometric phases due to the insufficient thermodynamic and phase diagram data (especially about the high-temperature δ-phase). The δ-, γ_1-, and γ_2- phases have been modeled as $(Co)_2(Zn)_{15}$, $(Co)_1(Zn)_7$, and $(Co)_1(Zn)_{13}$, respectively. Linear temperature dependence of their Gibbs energy values of formation ($\Delta^{\Phi}G^{f}$) has been accepted (Table 2).

4. Results and Discussion

The set of coefficients optimized through the programs THERMO-CALC and BINGSS [1995Luk] is shown in Table 2. By means of these coefficients, one can calculate the thermodynamic properties of all binary CoZn phases. A comparison between thermodynamic quantities calculated in this work and measured or assessed data is presented in Fig. 2-6. It is interesting to note that the largest enthalpies of formation in the system CoZn belong to the γ-phase region, while in the Ni-Zn system [2000Vas] they pertain to the equiatomic (β_1-phase) region.

According to the theoretical estimations of Niessen et al. [1983Nie], the largest magnitudes of the liquid phases enthalpies of formation in the systems Ni-Zn and Co-Zn are −34 and −19 kJ mol^{-1}, respectively, when referred to liquid metals. The pertinent values calculated with the optimized coefficients, however, are −13 and −8 kJ mol^{-1} (at 1750 K), respectively.

A compilation of experimental data, and those assessed in this work concerning the invariants and the special points of the Co-Zn phase diagram, is given in Table 3. It is worth noting that the hypothetical three-phase equilibrium α(Co) ↔ (εCo) + β_1 has been considered and calculated for the first time in this work. The same is valid for the enthalpies of the invariant reactions shown in Table 4.

The calculated phase diagram (valid for temperatures above 298.15 K) is presented in Fig. 7. The calculations have revealed (Table 3) that another formerly unknown invariant might exist at around 1015 K due to the three-phase equilibrium among α-ferromagnetic, α-paramagnetic, and β_1-phases. The estimated critical point of the related miscibility gap is situated at 1089 K and $X_{Zn} = 0.184$ (Fig. 7). The shape of this magnetically induced immiscibility region differs from the usual one. Such distorted miscibility gaps have relevance to the microstructural design of hard magnets [1995Nis].

The calculations show (Fig. 7) that the magnetic transition in the β_1-phase occurs at temperatures between 454 K (53.9 at.% Zn) and 410 K (57.1 at.% Zn). This result is in

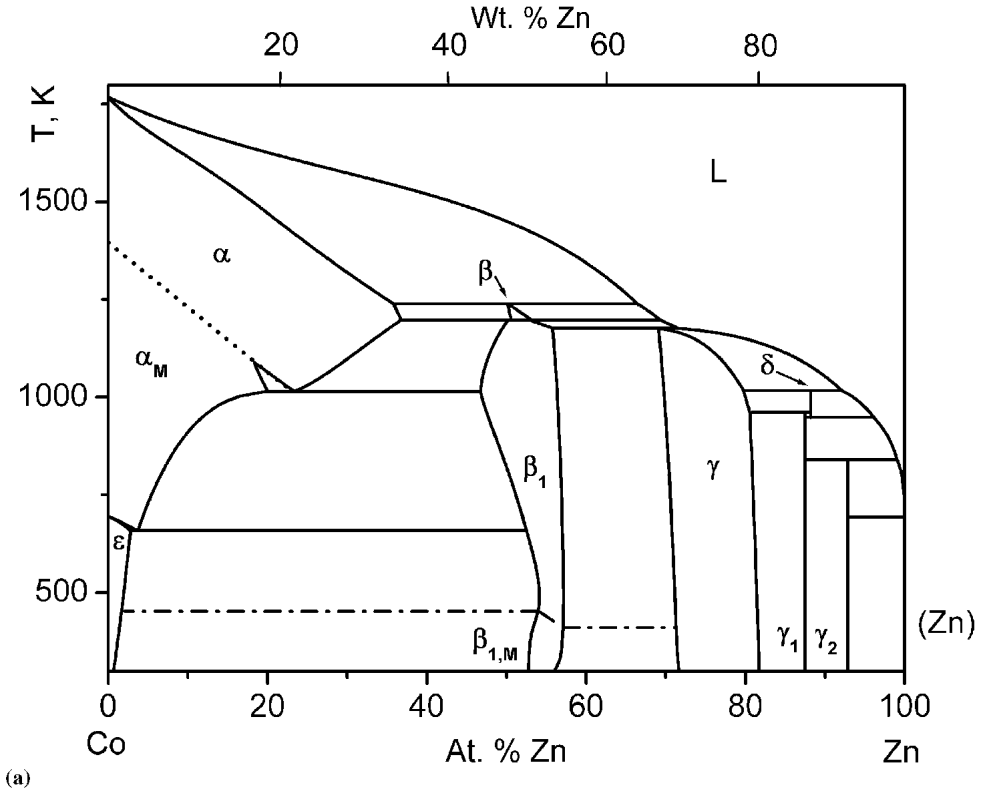

(a)

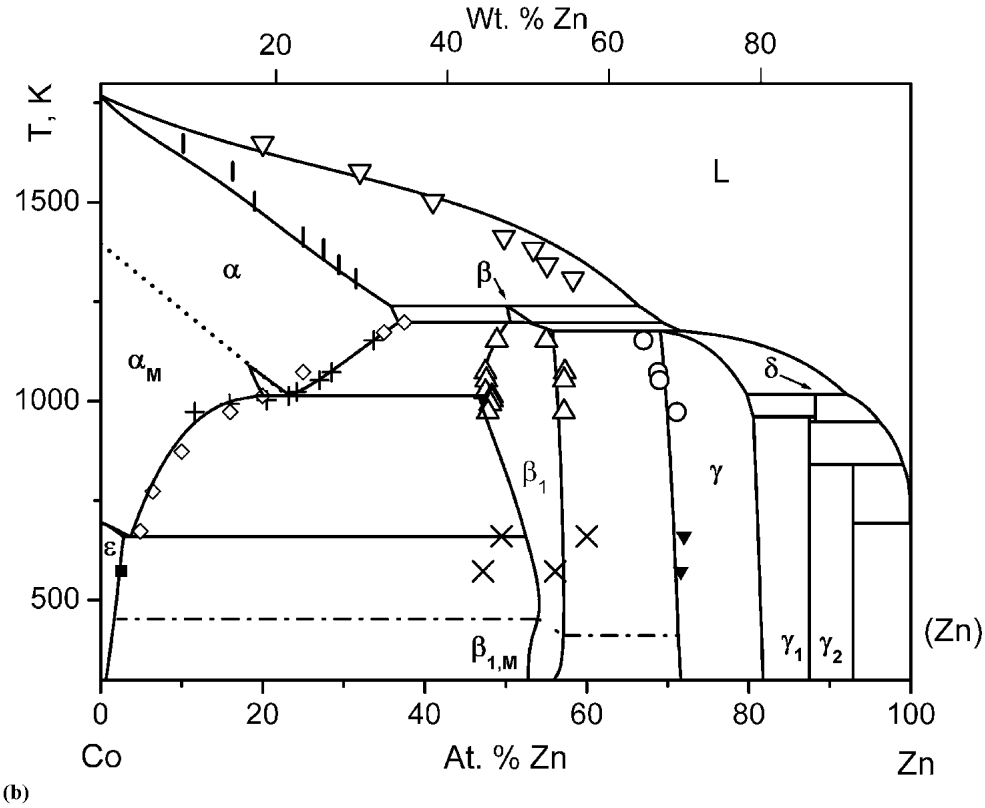

(b)

Fig. 7 (**a**) The calculated Co-Zn phase diagram. The small dots represent the T_C of the Co-based fcc solutions; and the line of dashes and dots represent the β_1-phase T_C. (**b**) The calculated Co-Zn equilibrium phase diagram with selected topological experimental data: data of Takayama et al. [1995Tak]: +, α and α_M; Δ, β_1; ○, γ. Data of Koster et al. [1937Kos]: *, ε; ◇, α and α_M. Data of Budurov and Vassilev [1976aBud]: ∇, liquid; I, α. Data of Lihl [1955Lih]: ■, ε. Authors' data: ×, β_1; and B, γ.

Table 5 Calculated Thermodynamic Properties Referred to H(SER, 298.15 K) (per Mole of Atoms) of the γ_1-phase ($CoZn_7$)

T (K)	Enthalpy ($J \cdot mol^{-1}$)	G ($J \cdot mol^{-1}$)	Entropy ($J \cdot mol^{-1} \cdot deg^{-1}$)	C_p ($J \cdot mol^{-1} \cdot deg^{-1}$)
298.15	−11 000	−21 900	36.5	25.4
371.81	−9 100	−24 800	42.2	26.0
445.48	−7 100	−28 100	47.0	26.8
519.14	−5 100	−31 700	51.1	27.5
592.81	−3 100	−35 600	54.8	28.4
666.47	−1 000	−39 800	58.2	29.3
740.14	1 200	−44 200	61.3	30.4
813.80	3 500	−48 800	64.3	30.9
887.47	5 800	−53 600	66.9	31.1
961.13	8 100	−58 700	69.4	31.3

Table 6 Calculated Thermodynamic Properties Referred to H(SER, 298.15 K) (per Mole of Atoms) of the γ_2-phase ($CoZn_{13}$)

T (K)	Enthalpy ($J \cdot mol^{-1}$)	G ($J \cdot mol^{-1}$)	Entropy ($J \cdot mol^{-1} \cdot deg^{-1}$)	C_p ($J \cdot mol^{-1} \cdot deg^{-1}$)
298.15	−6100	−18 000	39.8	25.4
358.38	−4600	−20 500	44.5	25.9
418.62	−3000	−23 300	48.6	26.5
478.85	−1400	−26 300	52.2	27.1
539.08	300	−29 600	55.4	27.8
599.32	2000	−33 000	58.4	28.5
659.55	4000	−36 600	61.1	29.2
719.78	5500	−40 400	63.7	30.2
780.02	7300	−44 300	66.2	30.8
840.25	9200	−48 300	68.5	31.1

Table 7 Calculated Thermodynamic Properties Referred to H(SER, 298.15 K) (per Mole of Atoms) of the δ-Phase (Co_2Zn_{15})

T (K)	Enthalpy ($J \cdot mol^{-1}$)	G ($J \cdot mol^{-1}$)	Entropy ($J \cdot mol^{-1} \cdot deg^{-1}$)	C_p ($J \cdot mol^{-1} \cdot deg^{-1}$)
298.15	−6 500	−18 700	41.1	25.4
377.97	−4 400	−22 300	47.2	26.1
457.78	−2 300	−26 300	52.3	26.9
537.60	−100	−30 600	56.7	27.7
617.41	2 100	−35 300	60.6	28.7
697.23	4 400	−40 300	64.1	29.7
777.04	6 850	−45 500	67.4	30.7
856.86	9 300	−51 000	70.4	31.1
936.67	11 800	−56 700	73.2	31.2
1016.49	14 300	−62 700	75.7	31.4

agreement with the measurements of Schramm [1941Sch] and Meyer and Taglang [1951Mey].

The assessed thermodynamic properties of the γ_1-, γ_2-, and δ-phases, are shown in Table 5, 6, and 7, respectively.

5. Conclusion

Thermodynamically consistent sets of coefficients have been derived enabling the calculation of the Co-Zn equilibrium diagram and the thermochemical properties of the binary phases. Generally, good agreement with the available experimental information has been achieved.

We would like to emphasize that most of the phase diagram data are rather ancient and that some of them might be uncertain (e.g., details concerning the high-temperature phases β and δ). The positions of the peritectic liquidus points are, in general, difficult to measure as well.

No direct thermochemical measurements concerning, for example, the enthalpies of formation, the enthalpies of the invariant reactions, and temperatures are known. The shape of the solvus at low temperatures and the homogeneity intervals of the solid phases also need further experimental studies. Thus, if new data become available, they could be used for verification and amendment to the present thermodynamic description.

Acknowledgment

The authors are grateful to the anonymous referees for their helpful advice.

References

1908Lew: K. Lewkonja: "Equilibria Between Liquid and Solid Zn-Rich Cobalt-Zinc Phases," *Z. Anorg. Chem.*, 1908, *59*, pp. 319-22.

1923Pie: W. Pierce and M. Palmerton: "Studies on the Constitution of Binary Zinc-Base Alloys," *Trans. AIME*, 1923, *68*, pp. 776-95.

1931Ekm: W. Ekman: "X-ray Studies of the Cobalt-Zinc Gamma-Phase," *Z. Physikal. Chem.*, 1931, *B12*, pp. 57-78.

1932Par: N. Parravano and V. Caglioti: "On the Structure of the Cobalt-Zinc Gamma-Phase," *Mem. Accad. Italia, Cl. Sci. Fis. Mat. Nat.*, 1932, *3*, pp. 1-21.

1937Has: U. Hashimoto: *Nippon Kinzoku Gakkai-Shi*, 1937, *1*, pp. 177-90.

1937Kos: W. Köster and E. Wagner: "Effect of the Elements Al, Ti, V, Cu, Zn, Sn and Sb on the Polimorphic Transition of the Cobalt," *Z. Metallkde*, 1937, *29*, pp. 230-32.

1938Sch1: J. Schramm: "The Cobalt-Zinc System," *Z. Metallkde.*, 1938, *30*, pp. 10-14.

1938Sch2: J. Schramm: "The Heats of Formation for the Three-Phase Transformations in the Binary Alloys of Zinc With Iron,

Cobalt, Nickel and Manganese," *Z. Metallkde*., 1938, *30*, pp. 131-35.

1938Sch3: J. Schramm: "X-Ray Investigation of Phase and Phase Limits of the Zinc Alloy Systems With Iron, Cobalt and Nickel," *Z. Metallkde*., 1938, *30*, pp. 122-30.

1938Sch4: J. Schramm: "The Magnetic Susceptibility of the Alloys of the Zinc With Nickel, Cobalt and Iron," *Z. Metallkde*., 1938, *30*, pp. 327-34.

1941Got: F. Gotzl, F. Halla, and J. Schramm: "δ_1 and ζ Phases in the Systems Fe-Zn and Co-Zn," *Z. Metallkde*., 1941, *33*, p. 375.

1941Sch: J. Schramm: "Co-Zn System," *Z. Metallkde*., 1941, *33*, pp. 46-48.

1944Paw: F. Pawlek: "Influence of Iron Metals on the Zinc Properties," *Z. Metallkde*., 1944, *36*, pp. 105-11.

1951Mey: A.J.P. Meyer and P. Taglang: "On the Ferromagnetism of the Beta-1 Phase of the Co-Zn Alloys," *Compt. Rend.*, 1951, *232*, pp. 1914-16.

1955Lih: F. Lihl and E. Weisberg: "Phase Boundaries in the System Co-Zn," *Z. Metallkde*., 1955, *46*, pp. 579-81.

1955Kos: W. Köster and H. Schmid: "The State of the Beta-Phase in the System Co-Zn," *Z. Metallkde*., 1955, *46*, pp. 468-69.

1958Han: M. Hansen and K. Anderko: *Constitution of Binary Alloys*, 2nd ed., McGraw-Hill, New York, NY, 1958, p. 1488.

1962Bro: P. Brown: "The Structure of the ζ-Phase in Transition Metal-Zinc Alloy Systems," *Acta Crystallogr.*, 1962, *15*, pp. 608-12.

1973Mel: V. Melikhov and A. Presnjakov: *Structure and Properties of Electron Phases*, Nauka, Alma-Ata, Kazakhstan, USSR, 1973 (in Russian).

1976Bud1: S. Budurov and G.P. Vassilev: "The Cobalt Side of the Phase Diagram Cobalt-Zinc," *Z. Metallkde*., 1976, *67*, pp. 170-72.

1976Bud2: S. Budurov, G.P. Vassilev, and L. Mandadjieva: "Thermodynamics of Cobalt-Zinc and Nickel-Zinc Austenites," *Z. Metallkde*., 1976, *67*, pp. 307-10.

1977Bud: S. Budurov and G.P. Vassilev: "Thermodynamics of the β- and γ-Phases in the Nickel-Zinc and Cobalt-Zinc Systems," *Z. Metallkde*., 1977, *68*, pp. 795-98.

1977Mor: A. Morton: "Inversion Domains in Gamma-brass Type Phases—Stabilization Mechanism—Role of Electron-Concentration," *Phys. Stat. Sol.(a)*, 1977, *44*, pp. 205-14.

1977Moz: A. Mozeva, D. Nenov, and N. Gidicova: "Determination of Activity of Zinc in Liquid Cobalt and Nickel-alloys," *Arch. Eisenhuettenwes.*, 1977, *48*, pp. 533-34.

1977Vas: G.P. Vassilev and S. Budurov: "Kinetics of Intermetallic Phase Layers Growth in the Co-Zn System," *Annual of the University of Sofia*, Faculty of Chemistry, 1977/1978, *72*, pp. 25-36.

1978Hil: M. Hillert and M. Jarl: "Model for Alloying Effects in Ferromagnetic Metals," *Calphad*, 1978, *2*, pp. 227-38.

1980Arn: L. Arnberg and S. Westman: "A Discussion of the Ordering in Some Vacancy-Containing Gamma Brasses," *Z. Kristallographie*, 1980, *152*, pp. 103-08.

1981Ali: S. Ali and V. Geiderich: "Thermodynamic Properties of Solid Co-Zn Alloys," *Zh. Fiz. Khim*. 1981, *67*, pp. 1248-51. (in Russian).

1981Ind: G. Inden: "The Role of Magnetism in the Calculation of Phase Diagrams," *Physica*, 1981, *103B*, pp. 82-100.

1981Pea: W.B. Pearson: "Vacancies and Atomic Ordering in Gamma Brasses of Ni, Pd, and Pt With Zn or Cd," *Z. Kristallographie*, 1981, *156*, pp. 281-94.

1982Com: H. Comert and J. Pratt: "The Thermodynamic Properties of Solid Cobalt-Zinc Alloys," *Thermoch. Acta*, 1982, *59*, pp. 267-85.

1983Bus: K.H.J. Buschow, P.G. van Engen, and R. Jongebreur: "Magneto-Optical Properties of Metallic Ferromagnetic Materials," *J. Magnetism Magn. Mater.*, 1983, *38*, pp. 1-22.

1983Nie: A.K. Niessen, A.R. Miedema, F.R. de Boer, and R. Boom: "Model Predictions for the Enthalpy of Formation of Transition Metal Alloys 2," *Calphad*, 1983, *7*, pp. 51-70.

1987Gui: A.F. Guillermet: "Critical Evaluation of the Thermodynamic Properties of Cobalt," *Intern. J. Thermod.*, 1987, *8*, pp. 481-510.

1990Nis: T. Nishizawa and K. Ishida: "The Cobalt System," *Bull. Alloy Phase Diagr.*, 1980, *4*, pp. 387-90.

1991Din: A.T. Dinsdale: "SGTE Data for Pure Elements," *CALPHAD*, 1991, *15*, pp. 317-425.

1991Ray: A. Ray, S. Smith, and J. Scofield: "Study of the Phase Transformation of Cobalt," *J. Phase Equilibria*, 1991, *12*, pp. 644-47.

1993Kow: M. Kowalski and P.J. Spencer: "Thermodynamic Reevaluation of the Cu-Zn System," *J. Phase Equilibria*, 1993, *14*, pp. 432-38.

1993Vas1: G.P. Vassilev: "Assessment of the Equilibrium between Solid and Liquid Cobalt-Zinc Solutions," *Cryst. Res. Technol.*, 1993, *28*, pp. 57-62.

1993Vas2: G.P. Vassilev and S. Budurov: "Growth Kinetics of Cobalt-Zinc Intermediate Phase Layers," *J. Alloys Compounds*, 1993, *199*, pp. 197-201.

1995Luk: H.L. Lukas, S. Fries, U. Kattner, and J. Weiss: *BINGGS, BINFKT*, Version 95-1, Max-Planck-Institute of Metall Science, Stuttgart, Germany, 1995.

1995Nis: T. Nishizawa: "Effect of Magnetic Transition on Phase Equilibria in Iron Alloys," *J. Phase Equilibria*, 1995, *16*, pp. 379-89.

1995Tak: T. Takayama, S. Shinohara, K. Ishida, and T. Nishizawa: "Anomalies in Phase Equilibria due to Magnetic Transition in Fe-Zn, Co-Zn and Fe-Co-Zn Systems," *J. Phase Equilibria*, 1995, *16*, pp. 390-95.

1996Mas: T. Massalski: *Binary Phase Diagrams* [CD-ROM], 2nd ed., 1996, ASM International, Materials Park, OH.

1996Rya: Yu.A. Ryabikin, V.D. Melikhov, and O.V. Zashkvara: "Paramagnetic Resonance Studies of the Co-Zn Gamma-Brass Structure," *The Physics of Metals and Metallography*, 1996, *81*(3), pp. 255-62 (translated from Russian).

2000Vas: G.P. Vassilev, T.G. Acebo, and J.-C. Tedenac: "Thermodynamic Optimization of the Ni-Zn System," *J. Phase Equilibria*, 2000, *21*, pp. 287-301.

2003Jia: M. Jiang, C.P. Wang, X.J. Liu, I. Ohnuma, R. Kainuma, G.P. Vassilev, and K. Ishida: "Thermodynamic Calculation of Phase Equilibria in Cu-Ni-Zn System," *J. Phys. Chem. Solids*. 2003 (in press)